

# Synthesis and biological evaluation of nonpeptide mimetics of $\omega$ -conotoxin GVIA

Jonathan B. Baell,<sup>a,b,\*</sup> Peter J. Duggan,<sup>c,\*,†</sup> Stewart A. Forsyth,<sup>a</sup> Richard J. Lewis,<sup>d</sup>  
Y. Phei Lok<sup>c</sup> and Christina I. Schroeder<sup>d</sup>

<sup>a</sup>Biomolecular Research Institute, 343 Royal Parade, Parkville, Vic 3052, Australia

<sup>b</sup>Structural Biology—Chemistry Group, The Walter and Eliza Hall, Institute of Medical Research, Biotechnology Centre,  
4 Research Avenue, La Trobe R & D Park, Bundoora, Vic 3086, Australia

<sup>c</sup>School of Chemistry, Monash University, Clayton, Vic 3800, Australia

<sup>d</sup>Institute of Molecular Bioscience, The University of Queensland, St. Lucia, Qld 4072, Australia

Received 7 April 2004; revised 28 May 2004; accepted 28 May 2004

Available online 24 June 2004

**Abstract**—A benzothiazole-derived compound (**4a**) designed to mimic the C $_{\alpha}$ –C $_{\beta}$  bond vectors and terminal functionalities of Lys2, Tyr13 and Arg17 in  $\omega$ -conotoxin GVIA was synthesised, together with analogues (**4b–d**), which had each side-chain mimic systematically truncated or eliminated. The affinity of these compounds for rat brain N-type and P/Q-type voltage gated calcium channels (VGCCs) was determined. In terms of N-type channel affinity and selectivity, two of these compounds (**4a** and **4d**) were found to be highly promising, first generation mimetics of  $\omega$ -conotoxin. The fully functionalised mimetic (**4a**) showed low  $\mu$ M binding affinity to N-type VGCCs (IC $_{50}$  = 1.9  $\mu$ M) and greater than 20-fold selectivity for this channel sub-type over P/Q-type VGCCs, whereas the mimetic in which the guanidine-type side chain was truncated back to an amine (**4d**, IC $_{50}$  = 4.1  $\mu$ M) showed a greater than 25-fold selectivity for the N-type channel.

© 2004 Elsevier Ltd. All rights reserved.

## 1. Introduction

$\omega$ -Conotoxins<sup>1</sup> are disulfide-rich peptides found in the venom of *Conus* snails.<sup>2,3</sup> The venom of these marine snails contains a large variety of peptides with diverse pharmacological properties.<sup>4–6</sup>  $\omega$ -Conotoxin GVIA (GVIA) is a 27-residue peptide from the fish-hunting cone snail *Conus geographus*. It is widely used as a biochemical probe in its capacity as a selective blocker of the N-type voltage gated calcium channel (VGCC), which also has the alternative designation, Ca $_v$ 2.2.<sup>7</sup> These calcium channels are found in the central and peripheral nervous systems. While inhibition of N-type VGCCs can aid in neuroprotection during ischemia,<sup>8–10</sup> our main interest in GVIA lies in its analgesic proper-

ties.<sup>11–14</sup> In fact, a related peptide from *Conus magus*,  $\omega$ -conotoxin MVIIA (MVIIA), known commercially as Ziconotide® and Prialt®, has entered phase III clinical trials<sup>15,16</sup> as an intrathecally administered, nonaddictive analgesic. Significantly, its use does not appear to lead to tolerance. Even though these conotoxins form relatively stable cysteine four-loop structures, which is a consequence of their three, intra-molecular disulfide bonds,<sup>17</sup> small-molecule nonpeptidic mimetics should possess enhanced stability in vivo. In addition, such compounds would be less likely to lead to allergic responses and their solubility properties could be engineered to provide greater potential for oral administration.

$\omega$ -Conotoxin GVIA, unlike MVIIA, is not considered a suitable therapeutic due to its essentially irreversible binding to the N-type VGCC.<sup>18</sup> Its high binding affinity, however, makes GVIA an attractive target for mimicry since this increases the likelihood of generating mimetics with potent activity. In addition, there is much structure-function data available on this peptide to facilitate mimetic design.<sup>14,19,20</sup> Several highly active, nonpeptidic N-type VGCC blockers are known.<sup>12,21</sup> These compounds

**Keywords:** Conotoxin; GVIA; Peptide mimetics; N-type calcium channels; Channel blocker.

\* Corresponding authors. Tel.: +61-3-9345-2108; fax: +61-3-9345-2211 (J.B.B.); tel.: +61-3-9545-2560; fax: +61-3-9545-2446 (P.J.D.); e-mail addresses: jbaell@wehi.edu.au; peter.duggan@csiro.au

† New address: CSIRO Molecular Science, Private Bag 10, Clayton South, Vic., 3169, Australia.

have resulted from optimisation of leads discovered by high-throughput screening, whereas we are specifically interested in rational mimetic design. Relevant to this approach, there have been a few reports of mimetics whose design has been influenced by a knowledge of the solution structure of MVIIA. Horwell and co-workers<sup>22–24</sup> in particular prepared three-residue mimetics of MVIIA built on a 1,3,5-trisubstituted benzene scaffold (**1a** and **1b**, Fig. 1), which proved to be potent inhibitors of the  $\text{Ca}^{2+}$  current in IMR-32 human neuroblastoma cells ( $\text{IC}_{50} = 3 \mu\text{M}$ ).<sup>24</sup> Dabak later described the synthesis of mimetics based on pyridine and benzene cores (**2** and **3**);<sup>25</sup> compounds designed to mimic the same residues of MVIIA as those targeted by Horwell. However, no biological data has so far been disclosed for these latter compounds.

The current dearth of nonpeptidic mimetics of  $\omega$ -conotoxins is a consequence of the nature of the pharmacophore defined for these highly constrained peptides.<sup>17,19</sup> In GVIA, for example, the residues identified as essential for activity are located disparately, undermining approaches that involve truncation of the natural peptide or its analogues. Little is known about the conformation of  $\omega$ -conotoxins when they are bound to the calcium channel, but it is possible that their spatial properties would remain largely unchanged from their solution structures, due to their relative rigidity. An exception may be the structural loop that contains a pivotal tyrosine residue (Tyr13), which could flex significantly on binding.

In terms of defining the  $\omega$ -conotoxin pharmacophore, a major role of the peptide backbone is to appropriately position the crucial side chains that ultimately interact with the calcium ion channel. The well-defined nature of the solution conformation of this backbone in GVIA and MVIIA has led to mimetic design efforts focused on the mimicry of side-chain projections, rather than the spatial disposition of the side-chain termini. We have previously tackled these design challenges and have

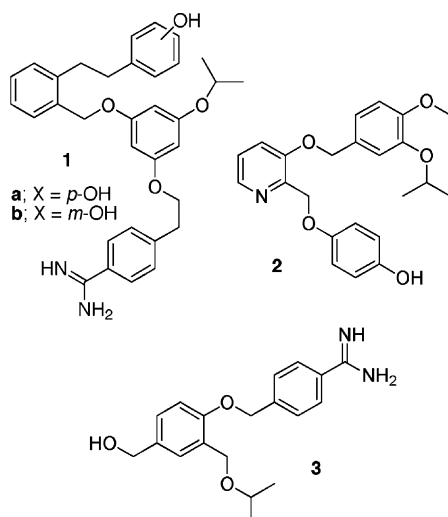


**Figure 1.** Previously reported type-III mimetics of  $\omega$ -conotoxin MVIIA.

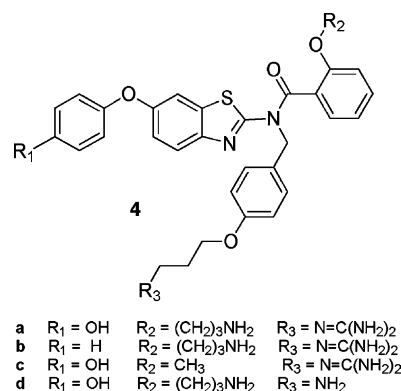


**Figure 2.** The structure of the type-III mimetic of  $\omega$ -conotoxin GVIA based on an aminobenzothiazole core (**4a**), along with the structures of three its analogues (**4b–d**).

proposed several type-III mimetics for the mimicry of Lys2, Tyr13 and Arg17 in GVIA.<sup>21,26</sup> We describe here the complete details of the synthesis of one of these proposed mimetics (**4a**, Fig. 2), a compound whose conformation is controlled by the properties of its aminobenzothiazole core, as well as three of its analogues (**4b–d**). In addition, the binding affinity of these compounds (**4a–d**) to N- and P/Q-type VGCCs is reported.

The decision to mimic the Lys2, Tyr13 and Arg17 residues of GVIA came about from an examination of the results of amino acid substitutions performed on GVIA itself. In particular, the outcomes of alanine scanning studies by Sato's group<sup>27</sup> and Norton and coworkers<sup>20</sup> indicate that Lys2 and Tyr13 are the most important determinants of the binding of GVIA to N-type VGCCs. Sato reported relative binding losses of approximately 20-fold, 170-fold and 1000-fold for the Lys2-Ala, Tyr13-Phe and Tyr13-Ala GVIA mutants, respectively, in chick brain synaptic plasma membranes. In general agreement with these findings, Norton's group recorded binding losses of around 50-fold and 215-fold, respectively, for the Lys2-Ala and Tyr13-Ala GVIA mutants in rat brain membrane preparations. The role of Arg17 in binding was also highlighted by the Arg17-Ala mutant of GVIA exhibiting a binding loss of around 6-fold compared to GVIA in a similar assay. Importantly, it was shown that the alanine replacements did not significantly perturb the solution tertiary structure of the peptide, confirming that the observed decreases in activity did not result from fundamental conformational changes. Taken together, these results underscore Lys2, Tyr13 and Arg17 as clear targets for mimetic design.

From our previous experimental and theoretical conformational analyses,<sup>26</sup> the core of the aminobenzothiazole system appeared likely to adopt a conformation in which certain of its bonds would closely mimic the spatial arrangement and direction of the  $\text{C}_\alpha\text{--C}_\beta$  bond projections of Lys2, Tyr13 and Arg17 in GVIA, as exemplified in Figure 3. In addition, an examination of a model of the proposed, fully functionalised mimetic (**4a**), overlaid on the GVIA structure in a similar way

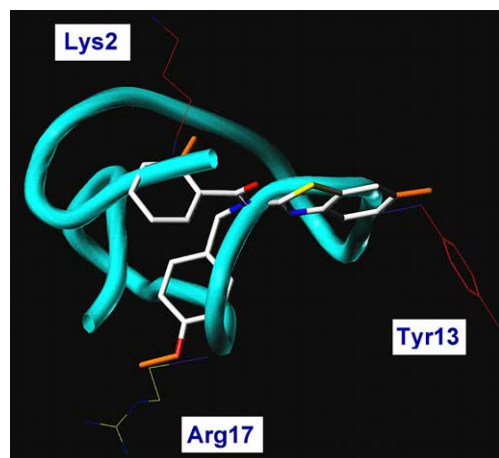


**Figure 3.** Three-dimensional picture of the benzothiazole scaffold 'core' superimposed on the NMR solution structure of  $\omega$ -conotoxin GVIA. The peptide backbone is shown in teal with residues Lys2, Tyr13 and Arg17 represented by thin lines. Orange portions of the scaffold represent the bonds that mimic the  $C_{\alpha}$ - $C_{\beta}$  bonds of the amino acid side chains in GVIA.

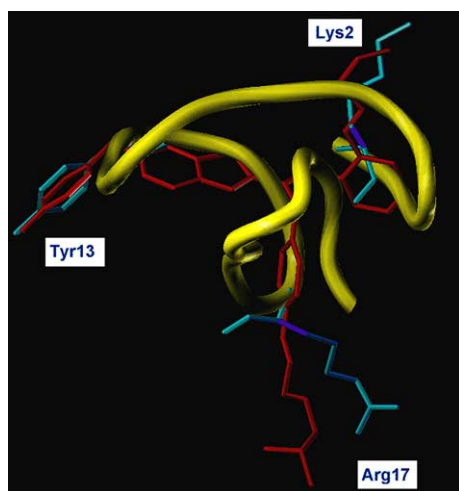


**Figure 4.** Backbone structure of  $\omega$ -conotoxin GVIA (yellow), with the side chains of Lys2, Tyr13 and Arg17 shown in teal ( $C_{\alpha}$ - $C_{\beta}$  bonds for Lys2 and Arg17 shown in purple, obscured for Tyr13), overlaid with a model of mimetic **4a** (red). Image taken from Ref. 1.

(Fig. 4) suggested that the terminal functionalities on the mimetic should also lie in close proximity to the termini of the three amino acid side chains **4a** is expected to mimic.

Analogues **4b–d** were included in the study to gain a better understanding of the possible contributions of the individual side-chain mimics to the biological activity of **4a**. These compounds possess alterations to the Lys2, Tyr13 and Arg17 side chains, respectively. In **4b**, the phenolic-OH group has been removed, converting the side chain from a Tyr to a Phe mimic. This mirrors Sato's work with Tyr13-Phe GVIA analogue,<sup>27</sup> mentioned above. In the case of the lysine side-chain mimic, its complete removal was not appropriate since this could affect the conformation of the scaffold, so the

*n*-propylamine substituent was instead replaced with a methoxy group to give **4c**. This alteration was thought to be the optimum way to study a change similar to the Lys2-Ala GVIA substitution examined by the groups of Sato and Norton.<sup>20,27</sup> The diamine, **4d**, in which the guanidyl group has been truncated to a primary amine, represents a readily accessible analogue of **4a**, being prepared from a precursor to **4a**.

Therapeutics that show greater binding selectivity for N-type VGCCs over P/Q-type channels, which are found at the neuromuscular junction, are highly desirable as they are expected to possess lower toxicity, a side effect that may be mediated through inadvertent P/Q-type blockade.<sup>28</sup> Therefore, the ability of **4a–d** to bind to both N-type and P/Q-type VGCCs was measured.

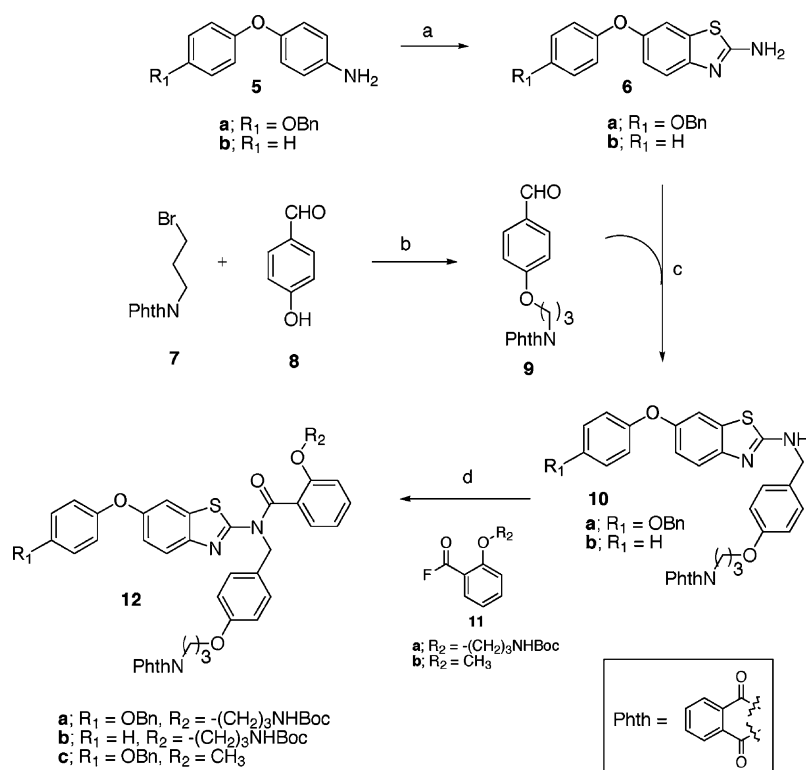
## 2. Results

### 2.1. Mimetic synthesis

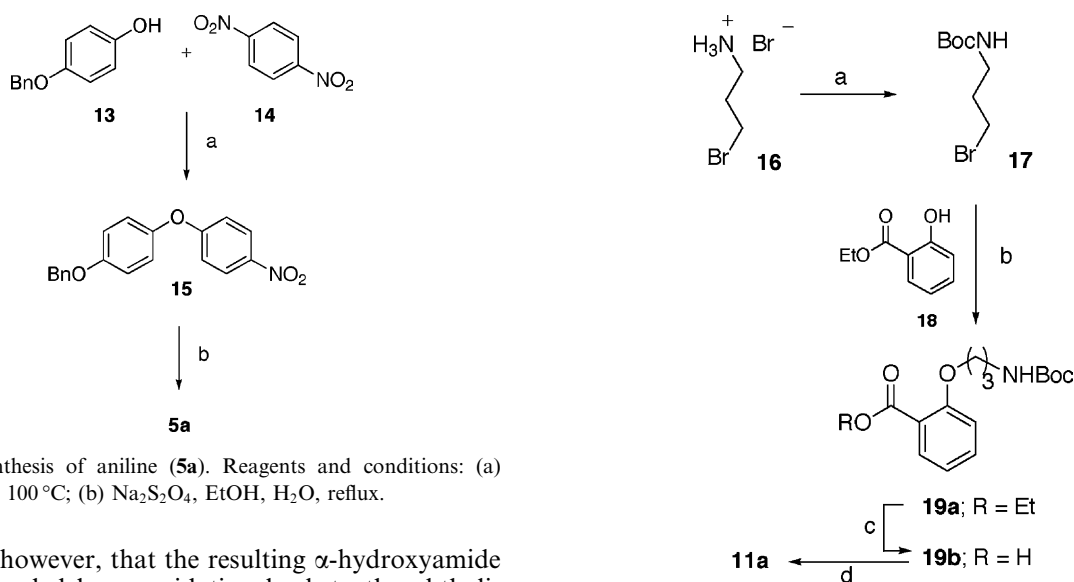
Broadly, the benzothiazole scaffold core was assembled via a convergent strategy, in three stages (Scheme 1). The benzothiazole ring system bearing the protected Tyr13 mimic (**6**), having been prepared from the corresponding aniline (**5**), was coupled, through a reductive amination to the precursor of the Arg13 mimic (**9**), to yield **10**. A salicylic acid fluoride derivative (**11**) bearing the protected Lys2 side-chain mimic was then appended through acylation of the secondary amine to give the key intermediate (**12**).

More specifically, 4-benzyloxyphenoxynitrobenzene (**15**, Scheme 2)<sup>29</sup> was prepared by arylation of 4-benzyloxyphenol (**13**) with 1,4-dinitrobenzene (**14**). Subsequent reduction with sodium hydrosulfite in refluxing aqueous ethanol provided the aniline derivative (**5a**). The benzothiazole core with the benzyl-protected Tyr13 mimic attached (**6a**), was then prepared via thiocyanation of **5a**. In this reaction ammonium thiocyanate and bromine were used to generate thiocyanogen in situ.<sup>30</sup> The formation of polythiocyanogen was minimised by exclusion of light from the reaction. A similar strategy was employed for the preparation of the phenyl analogue (**6b**), a precursor to the mimetic in which the Tyr13 hydroxyl group is absent (**4b**). In this case, the commercially available aniline (**5b**) was used as the starting point.

Alkylation of 4-hydroxybenzaldehyde (**8**) with the *N*-(3-bromopropyl)phthalimide (**7**) provided **9**.<sup>31,32</sup> This aldehyde was then separately coupled to each of the 2-aminobenzothiazoles (**6a** and **6b**) via imine formation in refluxing toluene, followed by reduction with sodium borohydride, to yield the secondary amines (**10a** and **10b**). One-pot reductive amination was not feasible as high temperatures and long reaction times were required to drive the formation of the imine to completion. Anhydrous conditions were crucial in the reduction step as the presence of water was found to lead to partial reduction of the phthalimide protecting group.<sup>33</sup> It was



**Scheme 1.** Convergent synthesis of key precursors (**12a-c**) to target mimetics (**4a-d**). Reagents and conditions: (a)  $\text{NH}_4\text{SCN}$ ,  $\text{Br}_2$ ,  $\text{HCO}_2\text{H}$ ,  $\text{CH}_3\text{CO}_2\text{H}$ ,  $-3-0^\circ\text{C}$ ; (b)  $\text{K}_2\text{CO}_3$ ,  $\text{CH}_3\text{CN}$ , rt; (c) (i) toluene, molecular sieves, reflux; (ii) dry, hot EtOH,  $\text{NaBH}_4$ ; (d) DIEA, THF,  $60^\circ\text{C}$ .



**Scheme 2.** Synthesis of aniline (**5a**). Reagents and conditions: (a)  $\text{K}_2\text{CO}_3$ , DMF,  $100^\circ\text{C}$ ; (b)  $\text{Na}_2\text{S}_2\text{O}_4$ , EtOH,  $\text{H}_2\text{O}$ , reflux.

also found, however, that the resulting  $\alpha$ -hydroxyamide could be recycled by re-oxidation back to the phthalimide (**10a** or **10b**) with PCC. Acylation of **10a** and **10b** with the appropriate acid fluorides (**11a** and **11b**) afforded the key intermediates (**12a-c**).

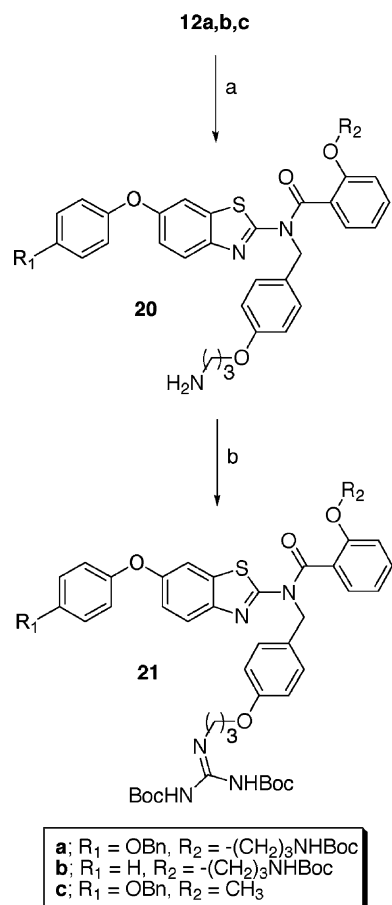
The preparation of the salicylic acid fluoride (**11a**) used in the synthesis of **12a** and **12b** is depicted in Scheme 3. The Lys2 side-chain precursor (**19a**) was prepared by the alkylation of ethyl salicylate (**18**) with Boc-protected 3-bromopropylamine (**17**). The ester functionality in **19a** was then hydrolysed to the corresponding carboxylic acid (**19b**) and converted to the acid fluoride (**11a**) with

**Scheme 3.** Synthesis of acid fluoride (**11a**) used to incorporate lysine side-chain precursor into **12a** and **12b**. Reagents and conditions: (a)  $\text{Boc}_2\text{O}$ , MeOH,  $\text{CH}_3\text{CN}$ ,  $\text{Et}_3\text{N}$ , rt; (b)  $\text{K}_2\text{CO}_3$ , DMF,  $50^\circ\text{C}$ ; (c) (i) NaOH, MeOH,  $\text{H}_2\text{O}$ , reflux; (ii) HCl, rt; (d) DAST,  $\text{CH}_2\text{Cl}_2$ , rt.

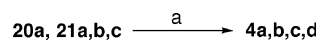
diethylaminosulfur trifluoride (DAST).<sup>34</sup> Anisic acid fluoride (**11b**) was prepared from anisic acid in a similar way, and used as the precursor for **4c**, where the Lys2 side-chain mimic is substituted with a methyl group. The use of an acid fluoride rather than the usual acid chloride derivative minimised in situ cleavage of the Boc

protecting group during the subsequent acylation of **10a** and **10b**.

The key intermediates (**12a–c**) were converted to the protected mimetics (**20a** and **21a–c**) by the route shown in Scheme 4. The phthalimide groups in (**12a–c**) were first cleaved by hydrazinolysis.<sup>35</sup> One of the products from these reactions, the amine (**20a**) was then deprotected with thioanisole/TFA<sup>38</sup> to afford **4d** (Scheme 5), the mimetic with the Arg17 guanidine functionality replaced with an amino group. The amines (**20a–c**) were then guanidylated by treatment with 1-*H*-pyrazole-1-*N,N'*-bis(*tert*-butoxycarbonyl)]carboxamide<sup>36</sup> to afford **21a–c**. The lead compound (**4a**) possessing Lys2, Tyr13 and Arg17 side-chain mimics, as well as the mimetic with the Lys2 mimic removed (**4c**), were obtained by treatment of **21a** and **21c** with thioanisole/TFA.<sup>38</sup> In both cases, prolonged treatment (8 h) with thioanisole/TFA was required in order to remove both of the Boc protecting groups of the guanidinium moiety. Deprotection of **21b**, which only possesses Boc protecting groups, was initially attempted using 4 M HCl in ethyl acetate,<sup>37</sup> but this method resulted in degradation. LC-MS of the reaction mixture revealed that cleavage at one or both carbon–nitrogen bonds of the tertiary amide had occurred. The mimetic in which the Tyr13 side-



**Scheme 4.** Conversion of key intermediates (**12a–c**) into fully protected mimetics (**18a–c**). Reagents and conditions: (a) N<sub>2</sub>H<sub>4</sub>·H<sub>2</sub>O, EtOH, reflux; (b) 1-*H*-pyrazole-1-*N,N'*-bis(*tert*-butoxycarbonyl)]carboxamide, DCM, rt.



**Scheme 5.** Deprotection reactions used to liberate fully de-protected mimetics (**4a–d**). Reagents and conditions: (a) For preparation of **4a**, **4c** and **4d**; thioanisole, TFA, rt; for the preparation of **4b**; TFA, rt.

chain mimic was replaced with a phenylalanine mimic (**4b**) was successfully obtained, however, with a simple treatment of **21b** with TFA.

Following the final deprotection steps, excess TFA was removed from the reactions mixtures under reduced pressure then the thioanisole was efficiently removed by repeated washing with hexane and a 2:1 mixture of ether and hexane. The resulting viscous liquids were dissolved in methanol or water and centrifuged to remove any insoluble components. The supernatants were freeze-dried to give white, hygroscopic solids (**4a–d**) in greater than 95% purity. After preliminary assays, the two most active compounds **4a** and **4b** were further purified by preparative HPLC to greater than 99% purity, then re-assayed.

## 2.2. Mimetic binding affinity for N- and P/Q-type VGCCs

The affinities of compounds **4a–d** for rat brain N-type and P/Q-type VGCCs were determined using a previously described competitive radioligand binding assay.<sup>39</sup> Thus, to measure the affinity of each of the mimetics for the N-type channel, <sup>125</sup>I-labelled ω-conotoxin GVIA was displaced from rat brain membrane using a range of mimetic concentrations, and the radioactivity of the residual membrane counted. ω-Conotoxin MVIIC is known to bind to the P/Q-type VGCC preferentially, so a similar approach, this time using <sup>125</sup>I-labelled ω-conotoxin MVIIC, was used to determine P/Q-type channel affinities. Representative binding curves are shown in Fig. 5 and the IC<sub>50</sub> values and channel selectivities (ΔpIC<sub>50</sub>) are shown in Table 1.

As Table 1 shows, the lead compound (**4a**) exhibited an IC<sub>50</sub> of 1.9 μM for the N-type VGCC, an outstanding result given the simplicity of this compound. As expected, the side-chain-altered analogues **4b–d**, were found to be less active than **4a**, with the most pronounced reduction in affinity being observed for **4c**. This compound showed a binding strength more than 50-fold weaker than that of **4a**, an observation that clearly marks the importance of the Lys2 side chain in binding to this ion channel. This observed drop in binding affinity for **4c** is of a similar order to that found for the Lys2-Ala peptide analogue of GVIA.<sup>20,27</sup> In contrast, the removal of the phenolic-OH was accompanied by only a slight decrease in binding affinity, with **4b** having a 2-fold weaker affinity for the rat N-type VGCC than **4a**. While this drop in activity suggests some degree of favourable interaction between the phenolic-OH and the N-type VGCC, it is nevertheless minute compared with the 170-fold binding potency loss observed by Sato and co-workers in the Tyr13-Phe GVIA analogue.<sup>20</sup> It thus appears that the phenolic hydroxyl group of the tyrosine mimic in **4a** does not contribute as much to its binding

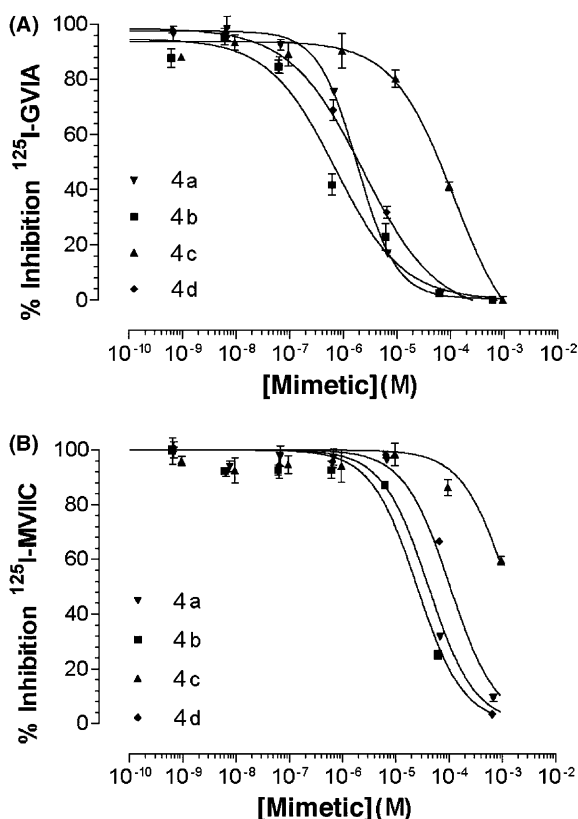


**Figure 5.** Mimetic potency at N-type and P/Q-type VGCCs in rat brain. (A), potency at N-type VGCCs measured by displacement of <sup>125</sup>I-GVIA. (B), potency at P/Q-type VGCCs measured by displacement of <sup>125</sup>I-MVIIC. Assays were run in triplicate for each dilution. Error bars represent the standard error of each mean (SEM).

affinity to N-type VGCC as the –OH does on the Tyr13 of GVIA. Similarly, the binding affinity of **4d**, in which the guanidine in **4a** has been truncated back to an amine, was also only approximately 2-fold lower than that of **4a**. This could result from the primary ammonium functionality accessing the Arg17 binding site, an effect commonly observed in protein–protein interactions. A classical example of this occurs in the trypsin-type serine proteases, which bind both the arginine and lysine side chains in their S<sub>1</sub> binding sites.

As far as P/Q-type channel affinities are concerned, all of the mimetics tested (**4a–d**) showed weaker affinities for this sub-type than for the N-type channel. This effect was most pronounced for the di-amino analogue (**4d**), which was 25 times less potent at the P/Q-type channel than at the N-type, and the fully functionalised mimetic

(**4a**), which was found to be 20 times less potent. The removal of the lysine side-chain mimic meant that **4c** showed very low affinity for the P/Q-type channel, now in the mM range. Interestingly, the des-OH analogue (**4b**), despite showing reduced affinity for the N-type VGCC relative to **4a**, actually bound more strongly to the P/Q-type VGCC than **4a**, and displayed low (7 fold) N-type VGCC selectivity. MVIIC, like most ω-conotoxins,<sup>1</sup> also has a tyrosine at position-13, but this new result suggests that the Tyr13-Phe mutant of MVIIC might show enhanced P/Q-affinity compared with the natural peptide.

### 3. Discussion

As has been done here, alanine scanning data is often used to identify the side chains that are most important in peptide–protein associations, and these side chains thus become the most obvious targets for mimetic design. Such an approach appears to be vindicated by the results presented here. However, it is important to affirm that the binding thermodynamics of peptide side chains could be very different from those in their mimetic counterparts. For example, we have found here that mimetic **4a** is only twice as active as its des-OH analogue **4b** in a radioligand binding assay, which, as mentioned above, is a negligible loss of potency when compared directly with the 170-fold potency loss observed with the Tyr13-Phe GVIA mutant.<sup>27</sup> There could be several reasons for this outcome. Firstly, it is possible that the phenol of **4a** engages a different subsite in the channel to that of Tyr13 in GVIA so that the phenolic-OH becomes relatively less important for the mimetic's binding. Alternatively, the higher pK<sub>a</sub> of the phenolic hydroxyl in the electron-rich mimetic may lead to a weaker interaction with the hydrogen bond acceptors on the N-type VGCC. However, such considerations are likely to be secondary when compared to solvation effects, which alone could account for the observed binding differences. The phenol in **4a** is highly solvent exposed and likely to be more so than its equivalent in GVIA, which is flanked by neighbouring residues. The de-solvation of the phenolic hydroxyl to form hydrogen bonds with the N-type VGCC may produce a greater penalty on binding than that for the Tyr13 in GVIA, thereby effectively diminishing the strength of its interaction with channel. Correspondingly, it is possible that the hydrophobic driving force for the burial of the phenyl ring in **4b** is greater than that for its counterpart in the Tyr13-Phe GVIA mutant.

**Table 1.** Potency (*M*) and selectivity ( $\Delta pIC_{50}$ ) of GVIA, MVIIC and mimetics **4a–d** of inhibition of <sup>125</sup>I-GVIA (N-type) or <sup>125</sup>I-MVIIC (P/Q-type) binding to rat brain VGCC's (95% confidence intervals shown in parentheses)

Compound	IC <sub>50</sub> (N-type)	pIC <sub>50</sub> (N-type)	IC <sub>50</sub> (P/Q-type)	pIC <sub>50</sub> (P/Q-type)	$\Delta pIC_{50}$
GVIA	3.0 × 10 <sup>-11</sup> (2.4 × 10 <sup>-11</sup> –3.7 × 10 <sup>-11</sup> )	10.52 (10.60–10.43)	1.2 × 10 <sup>-6</sup> (9 × 10 <sup>-5</sup> –1.4 × 10 <sup>-6</sup> )	5.92(6.05–5.85)	4.60
MVIIC	7.0 × 10 <sup>-9</sup> (5.3 × 10 <sup>-9</sup> –9.7 × 10 <sup>-9</sup> )	8.15 (8.28–8.01)	3.3 × 10 <sup>-10</sup> (2.4 × 10 <sup>-10</sup> –4.4 × 10 <sup>-10</sup> )	9.48 (9.62–9.35)	–1.33
<b>4a</b>	1.9 × 10 <sup>-6</sup> (1.6 × 10 <sup>-6</sup> –2.3 × 10 <sup>-6</sup> )	5.71 (5.78–5.63)	4.2 × 10 <sup>-5</sup> (3.4 × 10 <sup>-5</sup> –5.3 × 10 <sup>-5</sup> )	4.37 (4.47–4.28)	1.34
<b>4b</b>	3.8 × 10 <sup>-6</sup> (2.9 × 10 <sup>-6</sup> –4.9 × 10 <sup>-6</sup> )	5.42 (5.53–5.30)	2.6 × 10 <sup>-5</sup> (2.0 × 10 <sup>-5</sup> –3.2 × 10 <sup>-5</sup> )	4.59 (4.69–4.49)	0.83
<b>4c</b>	9.7 × 10 <sup>-5</sup> (8.7 × 10 <sup>-5</sup> –10.9 × 10 <sup>-5</sup> )	4.01 (4.06–3.96)	1.9 × 10 <sup>-3</sup> (1.5 × 10 <sup>-3</sup> –2.4 × 10 <sup>-3</sup> )	2.72 (2.82–2.62)	1.29
<b>4d</b>	4.1 × 10 <sup>-6</sup> (3.6 × 10 <sup>-6</sup> –4.9 × 10 <sup>-6</sup> )	5.38 (5.46–5.31)	1.0 × 10 <sup>-4</sup> (8.5 × 10 <sup>-5</sup> –1.3 × 10 <sup>-4</sup> )	3.98 (4.07–3.89)	1.40

Another interpretation of this situation follows from the prediction that the loss of rotational and translational entropy that occurs on binding a typical mimetic leads to a thermodynamic penalty of ca. 50–70 kJ/mol.<sup>40</sup> An IC<sub>50</sub> value of ca. 1 μM (IC<sub>50</sub> is equiv to K<sub>diss</sub>) corresponds to a free energy of binding of ca. –36 kJ/mol under physiological conditions. Thus, one could postulate that the side chains in **4a** contribute approximately 86–106 kJ/mol to the binding process. This is clearly inconsistent with any such interpretation based on the alanine scanning data from Norton's group<sup>20</sup> for Lys2-Ala, Tyr13-Ala and Arg17-Ala GVIA analogues, from which it could be concluded that the respective 50-fold, 215-fold and 6-fold binding potency losses infer energetic contributions from the Lys2, Tyr13 and Arg17 side chains of 10+14+5 = 29 kJ/mol in GVIA. While this thermodynamic analysis is relatively simplistic, it serves to illustrate the point that in the present case, it seems likely that one or more of the side chains in this series of compounds (**4a–d**) contributes significantly more energy to the binding process than would be expected from GVIA alanine scanning data alone.

The recognition of the above possibilities suggests that it is unwise to attempt to reconcile too closely peptide–protein binding data with that obtained from the binding of the corresponding small-molecule peptide mimetics.

#### 4. Conclusion

Compound **4a** comprises a benzothiazole-based scaffold designed to mimic the C<sub>α</sub>–C<sub>β</sub> projections of the Lys2, Tyr13 and Arg17 side chains in GVIA, residues, which are thought to interact favourably with N-type VGCCs on binding.<sup>19,20,27</sup> Though simplistic, in that the remaining 24 residues of GVIA are not represented, **4a** was found to bind to N-type VGCCs quite strongly with a low micromolar IC<sub>50</sub> while possessing some selectivity for this VGCC. Abolition of the Lys2 side chain mimic to give **4c** led to large decreases in binding at both the N- and P/Q-type VGCCs but modifications to the Tyr13 and Arg17 side chain mimics did not significantly affect binding to these ion channels. The analogue bearing the primary amine instead of a guanidinium moiety (**4d**) showed strong binding and high selectivity for the N-type VGCC and is a promising lead for further development of ω-conotoxin GVIA mimetics. We propose that the binding of **4a**, **4b** and **4d** to N- and P/Q-type VGCCs do indeed mimic the interactions of Lys2, Tyr13, and Arg17 side chains of GVIA as intended by the design. The notable N-type VGCC selectivity observed for **4a** and **4d** further implies apparent mimicry of this highly N-type selective peptide. Future work will include an examination of the effect of individually removing the Tyr13 and Arg17 side-chain mimics from **4a**.

Despite the impressive results presented here, improvement in binding by at least two orders of magnitude is still required to confer therapeutic relevance to these

mimetics. To this end, it is advantageous that **4a** is highly optimisable in that it contains convenient synthetic junction points for side-chain modifications, especially in the highly flexible Lys2 and Arg17 mimetic side chains. Appropriate conformational constraint of these two side chains alone might greatly increase potency. Since **4a** is intrinsically selective for N-type VGCCs over P/Q-type VGCCs, one would expect that this selectivity could concomitantly be increased further in subsequent optimisation cycles.

It is thought that binding to N-type VGCCs by GVIA leads to functional inhibition by reduction of Ca<sup>2+</sup> ion flux through physical occlusion of the ion channel pore. Thus, strength of binding does not necessarily correlate with functional inhibition, and while preliminary tests on **4a** indicated weak functional blockade of N-type VGCCs,<sup>26</sup> assessment of functional inhibition will need to be included in the optimisation cycle.

#### 5. Experimental

All commercially obtained chemicals and reagents were used as received. Melting points were recorded on a Reichert hot stage melting point apparatus. <sup>1</sup>H and <sup>13</sup>C nuclear magnetic resonance (NMR) spectra were recorded on a Varian Mercury 300 MHz spectrometer using the solvents specified. FTIR were run on Perkin–Elmer 1600 Series FTIR. ATR IR spectra were run on a Bruker IFS 55 FTIR Specac single reflection ATR system fitted with a single bounce diamond top plate. HRMS of compounds were recorded on a Bruker Bio-Apex 47e Fourier Transform mass spectrometer. Low Resolution MS was recorded on a Micromass Platform II mass spectrometer. The compounds analysed were dissolved in organic solvent and ionised using an electrospray ionisation source. MS data are recorded as positive electrospray ions unless indicated by (ESI–) where negative ions are reported. MS data from electron impact ionisation methods are indicated as 'EI-MS'. Elemental analyses were conducted by CMAS Chemical and Micro Analytical Services Pty. Ltd (P.O. Box 248, Belmont, Victoria, Australia 3216). HPLC purification of compounds **4a** and **4b** was carried out by Auspep Pty. Ltd (P.O. Box 806, Parkville, Victoria, Australia 3052).

##### 5.1. 1-(4-Benzyloxyphenoxy)-4-nitrobenzene (15)

4-Benzyloxyphenol (**13**) (6.87 g, 34 mmol) was heated at 100 °C with 1,4-dinitrobenzene (**14**) (4.95 g, 30 mmol) and K<sub>2</sub>CO<sub>3</sub> (23 g, 170 mmol) in DMF (80 mL) for 17 h. The reaction mixture was allowed to cool to room temperature, then poured into water (200 mL). The crude product was filtered out and triturated with water (100 mL), filtered again, then washed with MeOH (30 mL). Drying overnight in a vacuum oven afforded **15** (9.02 g, 93%) as a yellow solid. mp 179–180 °C (lit.<sup>29</sup> mp 110–112 °C); <sup>1</sup>H NMR (300 MHz, CDCl<sub>3</sub>) δ ppm: 5.08 (s, 2H), 6.97 (d, 2H, *J* = 9.3 Hz), 7.03 (s, 4H), 7.35–7.47 (m, 5H), 8.18 (d, 2H, *J* = 9.3 Hz); <sup>13</sup>C NMR (75 MHz,

$\text{CDCl}_3$ )  $\delta$  ppm: 70.5, 116.3, 116.4, 121.8, 125.9, 127.5, 128.1, 128.7, 136.7, 142.4, 148.1, 156.4, 164.1; ATR (neat)  $\text{cm}^{-1}$ : 3109, 3082, 3036, 2944, 2875, 1503, 1487, 1345; MS  $m/z$  344 ( $\text{M}+\text{Na}^+$ ).

### 5.2. 4-(4-Benzyloxyphenoxy)-aniline (5a)

The nitrobenzene (**15**) (3.48 g, 10 mmol) was dissolved in boiling EtOH (200 mL) and  $\text{Na}_2\text{S}_2\text{O}_4$  (9.4 g, 50 mmol) was added in four portions with water (20 mL). The resulting mixture was refluxed overnight. After cooling, the reaction mixture was concentrated to half volume, and the resulting light yellow precipitate was filtered out and suspended in 2 M HCl (100 mL). 2 M NaOH (250 mL) was added to the precipitate and the mixture was allowed to flocculate. The precipitate was again filtered out, washed with water and dried in a vacuum oven overnight to give **5a** (2.61 g, 83%) as a beige coloured powder. mp 140–142 °C (lit.<sup>29</sup> 132–135 °C);  $^1\text{H}$  NMR (300 MHz,  $\text{CDCl}_3$ )  $\delta$  ppm: 3.54 (s, 2H), 5.03 (s, 2H), 6.65 (d, 2H,  $J = 8.7$  Hz), 6.83 (d, 2H,  $J = 8.7$  Hz), 6.89 (s, 4H), 7.32–7.44 (m, 5H);  $^{13}\text{C}$  NMR (75 MHz,  $\text{CDCl}_3$ )  $\delta$  ppm: 70.6, 115.8, 116.2, 118.9, 120.1, 127.5, 127.9, 128.6, 137.2, 142.0, 150.0, 152.4, 154.3; ATR IR(neat)  $\text{cm}^{-1}$ : 3441, 3396, 3061, 3042, 3014, 2949, 2923, 1494; MS  $m/z$  292 ( $\text{M}+\text{H}^+$ ), 332 ( $\text{M}+\text{K}^+$ ).

### 5.3. 2-Amino-6-(4-benzyloxyphenoxy)-benzothiazole (6a)

Following a general procedure for the preparation of aminobenzothiazoles described by Nagarajan et al.,<sup>30</sup> the aniline (**5a**) (0.19 g, 0.67 mmol) and  $\text{NH}_4\text{SCN}$  (0.19 g, 2 mmol) were dissolved in a 20% formic acid-glacial acetic acid mixture (20 mL) and cooled to –3 °C with stirring, under  $\text{N}_2$ . With the exclusion of light from the reaction mixture, bromine (0.05 mL dissolved in 5 mL glacial acetic acid) was added dropwise over 1 h, while the reaction temperature was kept between –3 and 0 °C. The light shield was removed and the mixture was allowed to warm to room temperature overnight. Sodium hydroxide pellets and ice were added with stirring until pH 11 was attained, and the mixture was extracted with EtOAc (3 × 40 mL). The organic layer was separated and filtered through celite to remove polythiocyanogen ( $\text{SCN}$ )<sub>n</sub>. The organic layer was then washed with water (2 × 30 mL), saturated  $\text{NaHCO}_3$  (2 × 20 mL) and saturated brine (20 mL) then dried ( $\text{MgSO}_4$ ), filtered and concentrated to give a yellow solid. Recrystallising from toluene gave **6a** (0.197 g, 84%) as yellow needles. mp 167–168 °C;  $^1\text{H}$  NMR (300 MHz,  $\text{CDCl}_3$ )  $\delta$  ppm: 5.05 (s, 2H), 7.0–7.5 (m, 12H);  $^{13}\text{C}$  NMR (75 MHz,  $\text{CDCl}_3$ )  $\delta$  ppm: 110.4, 115.8, 117.3, 119.1, 120.0, 127.4, 127.9, 128.5, 131.4, 136.8, 145.9, 150.9, 153.8, 154.8, 165.5; ATR IR (neat)  $\text{cm}^{-1}$ : 3410, 3290, 3060, 6036, 2927, 2858; MS  $m/z$  349 ( $\text{M}+\text{H}^+$ ).

### 5.4. 2-Amino-6-phenoxybenzothiazole (6b)

The title compound was prepared from commercially available **5b** as described for the synthesis of **6a** to

give **6b** (4.707 g, 56%). mp 173–174 °C (lit.<sup>30</sup> mp 166–168 °C);  $^1\text{H}$  NMR (300 MHz,  $\text{CDCl}_3$ )  $\delta$  ppm: 5.49 (s, 1H), 6.97–7.12 (m, 4H), 7.30–7.36 (m, 3H), 7.52 (dd, 1H,  $J = 0.3, 8.7$  Hz);  $^{13}\text{C}$  NMR (75 MHz,  $\text{CDCl}_3$ )  $\delta$  ppm: 111.7, 118.1, 118.3, 119.7, 122.9, 129.6, 147.6, 152.3, 157.8, 164.9; FTIR (KBr)  $\text{cm}^{-1}$ : 3428, 3298, 3060, 2940; MS  $m/z$  243 ( $\text{M}+\text{H}^+$ ); HRMS calcd for  $\text{C}_{13}\text{H}_{10}\text{N}_2\text{OS}$  ( $\text{M}+\text{H}^+$ ) 243.0592, found 243.0559. Anal. Calcd for  $\text{C}_{13}\text{H}_{10}\text{N}_2\text{OS}$ : C, 64.40; H, 4.16; N, 11.56; S, 13.23. Found: C, 64.58; H, 4.10; N, 11.41; S, 13.17.

### 5.5. 4-(3-(1,3-Dihydro-1,3-dioxo-2H-isoindol-2-yl)propoxy)-benzaldehyde (9)

3-Bromo-*N*-propylphthalimide (**7**) (6.70 g, 2.5 mmol) and 4-hydroxybenzaldehyde (**8**) (3.36 g, 2.75 mmol) were stirred at room temperature with  $\text{K}_2\text{CO}_3$  (7.68 g, 3.75 mmol) in acetonitrile (60 mL) for 15 h. The reaction mixture was then poured into iced water (400 mL) with stirring and left to stand. The resulting white precipitate was filtered out, triturated with 2 M NaOH (2 × 30 mL) and water (50 mL). After a final filtration, recrystallisation from EtOAc gave **9** (4.16 g, 68%) as white needles. mp 131–132 °C (lit.<sup>31</sup> mp 127–128 °C);  $^1\text{H}$  NMR (300 MHz,  $\text{CDCl}_3$ )  $\delta$  ppm: 2.22 (p, 2H,  $J = 6.3$  Hz), 3.92 (t, 2H,  $J = 6.6$  Hz), 4.12 (t, 2H,  $J = 6.3$  Hz), 6.88 (d, 2H,  $J = 8.7$  Hz), 7.71–7.85 (m, 6H), 9.86 (s, 1H);  $^{13}\text{C}$  NMR (75 MHz,  $\text{CDCl}_3$ )  $\delta$  ppm: 28.2, 35.4, 66.1, 114.7, 123.3, 129.9, 131.8, 132.0, 133.9, 163.5, 168.2, 190.5; FTIR (KBr)  $\text{cm}^{-1}$ : 3071, 2928, 2857, 2786, 2690, 1857, 1714; MS  $m/z$  332 ( $\text{M}+\text{Na}^+$ ); EI-MS  $m/z$  309, 189, 188, 161, 160, 104, 77; HRMS calcd for  $\text{C}_{18}\text{H}_{15}\text{NO}_4$  ( $\text{M}+\text{Na}^+$ ) 332.0899, found 332.0893.

### 5.6. 2-(3-(4-((6-(4-Benzyloxy-phenoxy)-benzothiazol-2-ylamino)-methyl)-phenoxy)-propyl)-isoindole-1,3-dione (10a)

The aldehyde (**9**) (0.422 g, 1.38 mmol) and the amino-benzothiazole (**6a**) (0.477 g, 1.38 mmol) were refluxed with 4 Å molecular sieves in toluene (45 mL) under  $\text{N}_2$  overnight. The resulting bright yellow imine solution was added to a mixture of  $\text{NaBH}_4$  (0.15 g, 6.9 mmol) in excess hot, dry EtOH (100 mL). The resulting mixture was allowed to cool with stirring under  $\text{N}_2$ , then concentrated under reduced pressure. The resulting solid was washed with EtOH to afford pure **10a** (0.607 g, 69%) as an off-white powder. mp 158.9–159 °C;  $^1\text{H}$  NMR (300 MHz,  $\text{CDCl}_3$ )  $\delta$  ppm: 2.18 (p, 2H,  $J = 6.5$  Hz), 3.90 (t, 2H,  $J = 6.8$  Hz), 4.02 (t, 2H,  $J = 5.9$  Hz), 4.51 (s, 2H), 5.05 (s, 2H), 6.96 (s, 2H), 6.77–7.85 (m, 20H);  $^{13}\text{C}$  NMR (75 MHz,  $\text{CDCl}_3$ )  $\delta$  ppm: 28.4, 35.5, 48.9, 65.7, 70.6, 110.6, 114.7, 115.8, 117.3, 119.4, 119.8, 123.2, 127.4, 127.9, 128.5, 129.0, 129.4, 131.3, 132.0, 133.8, 136.9, 148.0, 151.4, 152.9, 154.6, 58.3, 166.0, 168.2; ATR IR(neat)  $\text{cm}^{-1}$ : 3172, 3094, 3063, 3032, 2950, 2920, 2854, 1703; MS  $m/z$  642 ( $\text{M}+\text{H}^+$ ); HRMS calcd for  $\text{C}_{38}\text{H}_{31}\text{N}_3\text{O}_5\text{S}$  ( $\text{M}+\text{H}^+$ ) 642.2063, found 642.2060. Anal. Calcd for  $\text{C}_{38}\text{H}_{31}\text{N}_3\text{O}_5\text{S}$  requires C, 71.12; H, 4.87; N, 6.55; S, 5.00. Found C, 71.08; H, 4.88; N, 6.32; S, 5.03.

### 5.7. 2-(3-(4-((6-Phenoxy-benzothiazol-2-ylamino)-methyl)-phenoxy)-propyl)-isoindole-1,3-dione (**10b**)

The title compound was prepared from **6b** and **9** in a manner similar to that described for the preparation of **10a** to give **10b** (0.77 g, 64%). mp 189–190 °C; <sup>1</sup>H NMR (300 MHz, CDCl<sub>3</sub>) δ ppm: 2.18 (q, 2H, *J* = 6.6 Hz), 2.40 (s, 1H), 3.90 (t, 2H, *J* = 6.6 Hz), 4.11 (t, 2H, *J* = 6.6 Hz), 4.52 (s, 2H), 6.70–7.10 (m, 8H) 7.20–7.58 (m, 8H), 7.69–7.85 (m, 4H); <sup>13</sup>C NMR (75 MHz, CDCl<sub>3</sub>) δ ppm: 28.3, 35.5, 48.9, 65.7, 111.8, 114.6, 117.9, 118.3, 119.4, 122.6, 123.2, 128.9, 129.4, 129.6, 131.4, 133.0, 133.8, 148.6, 151.5, 158.1, 158.3, 166.3, 168.2; ATR IR (neat) cm<sup>-1</sup>: 3167, 3087, 3060, 3039, 2950, 2920, 2854, 1703; HRMS calcd for C<sub>31</sub>H<sub>25</sub>N<sub>3</sub>O<sub>4</sub>S (M+H<sup>+</sup>) 536.1644 found 536.1635. EI-HRMS *m/z* 188.0701, 165.0122, 160.0394.

### 5.8. *tert*-Butyl-*N*-(3-bromopropyl)-carbamate (**17**)

*tert*-Butoxycarbonyl anhydride (6.07 g, 27.8 mmol) was dissolved in MeOH:acetonitrile (50:50, 30 mL) and Et<sub>3</sub>N (7.7 mL, 55.6 mmol) was added with stirring. After 15 min 3-bromopropylamine hydrobromide (**16**) (3.43 g, 27.8 mmol) in MeOH:acetonitrile (50:50, 15 mL) was added dropwise at room temperature over 1.5 h. The solvents were then removed under reduced pressure and the residue dissolved in EtOAc (40 mL), washed with water (2×30 mL), and saturated brine (40 mL). After drying (MgSO<sub>4</sub>) the EtOAc was evaporated to give **17** (3.39 g, 91%) as a clear, viscous liquid (lit.<sup>41</sup> mp. 38–39 °C), which gave a positive test with ninhydrin stain. <sup>1</sup>H NMR (300 MHz, CDCl<sub>3</sub>) δ ppm: 1.43 (s, 9H), 2.04 (p, 2H, *J* = 6.3 Hz), 3.27 (q, 2H, *J* = 6.3 Hz), 3.43 (t, 2H, *J* = 6.3 Hz); <sup>13</sup>C NMR (75 MHz, CDCl<sub>3</sub>) δ ppm: 28.7, 31.2, 33.0, 39.3, 79.8, 156.1; FTIR (NaCl) cm<sup>-1</sup>: 3348, 2977, 2933, 1690; MS *m/z* 260 (M+Na<sup>+</sup>).

### 5.9. Ethyl-2-(3-(*tert*-butoxycarbonylamino)-propoxy)-benzoate (**19a**)

Ethyl salicylate (**18**) (2.3 mL, 15.7 mmol), K<sub>2</sub>CO<sub>3</sub> (8.6 g, 62.8 mmol) and the Boc-protected bromoamine (**17**) (3.67 g, 15.5 mmol) were stirred in DMF (35 mL) at 50 °C for 24 h. After allowing the reaction mixture to cool to room temperature, it was washed with a mixture of EtOAc (40 mL) and 1M HCl (40 mL). The organic layer was then removed and washed with 10% citric acid (2×40 mL), saturated NaHCO<sub>3</sub> (4×40 mL) and saturated brine (2×30 mL). After drying (MgSO<sub>4</sub>) and filtering, the solvent was evaporated under reduced pressure. The residue was purified by flash column chromatography using a 40:60 EtOAc:hexane eluent to give **19a** (4.74 g, 70%) as a viscous, yellow liquid. <sup>1</sup>H NMR (300 MHz, CDCl<sub>3</sub>) δ ppm: 1.37 (t, 3H, *J* = 6.9 Hz), 1.43 (s, 9H), 2.05 (p, 2H, *J* = 6.3 Hz), 4.10 (t, 2H, *J* = 5.7 Hz), 4.36 (q, 2H, *J* = 7.2 Hz), 5.89 (s, 1H), 6.92–7.00 (m, 2H), 7.41–7.47 (m, 1H), 7.83–7.86 (dd, 1H, *J* = 1.8, 7.8 Hz); <sup>13</sup>C NMR (75 MHz, CDCl<sub>3</sub>) δ ppm: 14.7, 28.8, 28.5, 39.4, 61.1, 68.1, 78.9, 112.9, 120.0, 120.4, 132.0, 133.8, 156.5, 158.7, 166.0; FTIR (NaCl) cm<sup>-1</sup>:

3361, 3200, 2978, 2934, 2932, 170; HRMS calcd for C<sub>17</sub>H<sub>25</sub>NO<sub>5</sub> (M+Na<sup>+</sup>) 346.1630, found 346.1623; Anal. Calcd for C<sub>17</sub>H<sub>25</sub>NO<sub>5</sub> requires C, 63.14; H, 7.79; N, 4.33; O, 24.74. Found: C, 63.16; H, 7.91; N, 4.37; O, 24.56.

### 5.10. 2-(3-(*tert*-Butoxycarbonylamino)-propoxy)-benzoic acid (**19b**)

The ethyl ester (**19a**) (4.74 g, 14.67 mmol) was heated with NaOH (1.76 g, 44 mmol) at reflux in 25% H<sub>2</sub>O/MeOH (50 mL) for 6 h. The solvents were then removed under reduced pressure to give a white solid. This solid was dissolved in ether (30 mL) and extracted with 2 M NaOH (3×30 mL). The basic aqueous layer was washed with ether (30 mL) and then acidified on ice with 3 M HCl to pH 1. This acidic aqueous solution was then extracted with ether (3×30 mL). The ethereal extracts were combined, washed with saturated brine (2×30 mL), dried (MgSO<sub>4</sub>), filtered and concentrated to give the desired acid (**19b**) (4.03 g, 93%) as a clear viscous liquid. <sup>1</sup>H NMR (300 MHz, CDCl<sub>3</sub>) δ ppm: 1.40 (s, 9H), 2.08 (p, 2H, *J* = 6.0 Hz), 3.36 (q, 2H, *J* = 6.0 Hz), 4.25 (t, 2H, *J* = 6.0 Hz), 5.89 (s, 1H), 6.92–7.00 (m, 2H), 7.41–7.47 (m, 1H), 7.83–7.86 (dd, 1H, *J* = 1.8, 7.8 Hz); <sup>13</sup>C NMR (75 MHz, CDCl<sub>3</sub>) δ ppm: 28.7, 30.0, 37.9, 67.7, 79.8, 112.7, 118.6, 121.9, 133.5, 134.8, 156.5, 157.8, 166.7; FTIR (NaCl) cm<sup>-1</sup>: 3500–2800, 3344, 3200, 3190, 2978, 2950, 2900, 1700; MS *m/z* 318 (M+Na<sup>+</sup>); HRMS calcd for C<sub>15</sub>H<sub>21</sub>NO<sub>5</sub> (M+Na<sup>+</sup>) 318.1317 found 318.1306.

### 5.11. 2-(3-(*tert*-Butoxycarbonylamino)-propoxy)-benzoyl fluoride (**11a**)

Following the general procedure for the preparation of acylfluorides reported by Kaduk et al.,<sup>34</sup> benzoic acid derivative (**19b**) (1.10 g, 3.7 mmol) was stirred at 25 °C with diethylaminosulfur trifluoride (DAST) (1 mL, 5.6 mmol) in dry DCM (15 mL) for 60 min. The resulting mixture was then washed with ice water (2×10 mL) and saturated brine (10 mL). The organic layer was dried (MgSO<sub>4</sub>), filtered, concentrated and exposed to high vacuum for 2 h to give **11a** (0.98 g, 90%) as a reddish brown viscous liquid. <sup>1</sup>H NMR (300 MHz, CDCl<sub>3</sub>) δ ppm: 1.43 (s, 9H), 2.06 (p, 2H, *J* = 5.9 Hz), 3.39 (q, 2H, *J* = 5.8 Hz), 4.16 (t, 2H, *J* = 5.7 Hz), 5.36 (s, 1H), 6.92–7.03 (m, 2H), 7.60 (m, 1H), 7.93–7.82 (dd, 1H, *J* = 1.5, 7.5 Hz); FTIR (NaCl) cm<sup>-1</sup>: 3406, 3200, 3190, 2978, 2960, 2900, 1811, 1702; MS *m/z* 330 (M+Na<sup>+</sup>), 595 (2M+H<sup>+</sup>).

### 5.12. Anisoyl fluoride (**11b**)

The title compound was prepared from commercially available anisic acid following the procedure described for the synthesis of **11a** (93 mg, 92%) and used immediately after preparation. <sup>1</sup>H NMR (300 MHz, CDCl<sub>3</sub>) δ ppm: 3.94 (s, 3H), 7.03 (m, 2H), 7.62 (m, 1H), 7.91 (dd, 1H, *J* = 1.2, 8.1 Hz). FTIR (NaCl) cm<sup>-1</sup>: 3083, 3011, 2949, 2843, 1816.

**5.13. *N*-(3-(2-((6-(4-Benzyloxy-phenoxy)-benzothiazol-2-yl)-(4-(3-(1,3-dihydro-1,3-dioxo-isoindol-2-yl)-propoxy)-benzyl)-carbamoyl)-phenoxy)-propyl)-carbamic acid *tert*-butyl ester (**12a**)**

The benzylamine (**10a**) (0.112 g, 174  $\mu$ mol), acid fluoride (**11a**) (0.103 g, 348  $\mu$ mol) and DIEA (0.17 mL, 696  $\mu$ mol) were stirred at 60 °C in THF (1 mL) overnight. DCM (10 mL) was then added to the cooled reaction mixture and the organic layer was washed with 10% citric acid (3  $\times$  5 mL) and treated with excess ethylene diamine. The DCM layer was then washed with saturated NaHCO<sub>3</sub> (5 mL) and brine (2  $\times$  5 mL). The organic layer was dried (MgSO<sub>4</sub>), filtered and evaporated to dryness. Purification by radial chromatography (1:4 EtOAc:DCM) afforded **12a** (0.112 g, 70%) as a brown amorphous solid. mp 62–65 °C (foam); <sup>1</sup>H NMR (300 MHz, CDCl<sub>3</sub>)  $\delta$  ppm: 1.39 (s, 9H), 1.83 (s, 2H), 2.13 (p, 2H, *J* = 6.3 Hz), 3.13 (s, 2H), 3.87 (t, 2H, *J* = 6.8 Hz), 3.94 (q, 4H, *J* = 6.0 Hz), 4.78 (br s, 1H), 5.06 (s, 2H), 5.53 (br s, 1H), 6.58–7.18 (m, 12H), 7.25–7.83 (m, 12H); <sup>13</sup>C NMR (75 MHz, CDCl<sub>3</sub>)  $\delta$  ppm: 28.3, 28.4, 29.4, 35.5, 37.5, 51.5, 65.6, 66.3, 70.5, 79.1, 109.4, 112.3, 114.0, 115.9, 117.5, 120.3, 120.9, 122.3, 123.1, 124.7, 127.4, 127.9, 128.1, 128.5, 128.7, 129.0, 131.5, 132.0, 133.8, 134.5, 136.8, 143.8, 150.8, 154.6, 154.9, 155.0, 155.9, 157.8, 158.7, 168.1, 169.5; ATR IR(neat) cm<sup>-1</sup>: 3394, 3057, 3022, 2969, 2934, 2875, 1707; HRMS calcd for C<sub>53</sub>H<sub>50</sub>N<sub>4</sub>O<sub>9</sub>S (M+H<sup>+</sup>) 919.3377, (M+Na<sup>+</sup>) 941.3196, found 919.3372, 941.3320.

**5.14. *N*-(3-(2-((4-(3-(1,3-Dihydro-1,3-dioxo-isoindol-2-yl)-propoxy)-benzyl)-6-(phenoxy-benzothiazol-2-yl)-carbamoyl)-phenoxy)-propyl)-carbamic acid *tert*-butyl ester (**12b**)**

The title compound was prepared from **10b** and **11a** in a manner similar to that as described for the synthesis of **12a**. Purification by radial chromatography using a 1:9 EtOAc:DCM eluant afforded **12b** (0.310 g, 45%) as a brown amorphous solid. mp 64–66 °C (glass); <sup>1</sup>H NMR (300 MHz, CDCl<sub>3</sub>)  $\delta$  ppm: 1.39 (s, 9H), 1.84 (s, 2H), 2.14 (p, 2H, *J* = 6.5 Hz), 3.15 (s, 2H), 3.87 (t, 2H, *J* = 6.8 Hz), 3.98 (q, 4H, *J* = 6.5 Hz), 4.81 (br s, 1H), 5.54 (br s, 1H), 5.10 (br s, 1H), 6.60 (m, 2H), 6.90–7.04 (m, 6H), 7.05–7.83 (m, 12H); <sup>13</sup>C NMR (75 MHz, CDCl<sub>3</sub>)  $\delta$  ppm: 28.3, 28.4, 29.4, 35.4, 37.5, 51.5, 65.6, 66.3, 79.1, 110.8, 112.3, 114.0, 118.4, 120.9, 122.3, 123.0, 123.1, 124.6, 128.1, 128.7, 129.0, 129.6, 131.5, 132.0, 133.8, 134.5, 144.3, 153.6, 154.6, 155.9, 157.6, 157.8, 159.0, 168.1, 169.5; FTIR (NaCl) cm<sup>-1</sup>: 3850–3490, 3409, 3060, 2976, 2960, 2955, 1771, 1704, 1661; MS *m/z* 813 (M+H<sup>+</sup>); HRMS calcd for C<sub>46</sub>H<sub>44</sub>N<sub>4</sub>O<sub>8</sub>S (M+H<sup>+</sup>) 813.2958, (M+Na<sup>+</sup>) 835.2778, found 813.2978, 835.2789.

**5.15. *N*-(6-(4-Benzyloxy-phenoxy)-benzothiazol-2-yl)-*N*-(4-(3-(1,3-dihydro-1,3-dioxo-isoindol-2-yl)-propoxy)-benzyl)-2-methoxy-benzamide (**12c**)**

The title compound was prepared from **10a** and **11b** in a manner similar to that as described for the synthesis of

**12a** to give **12c** (0.172 g, 58%) as a brown amorphous solid. mp 64–68 °C (glass); <sup>1</sup>H NMR (300 MHz, CDCl<sub>3</sub>)  $\delta$  ppm: 2.13 (p, 2H, *J* = 6.5 Hz), 3.72 (s, 3H), 3.87 (t, 2H, *J* = 6.0 Hz), 3.94 (t, 2H, *J* = 6.9 Hz), 6.61 (dd, 2H, *J* = 8.7 Hz), 6.86–7.15 (m, 9H), 7.30–7.83 (m, 12H); <sup>13</sup>C NMR (75 MHz, CDCl<sub>3</sub>)  $\delta$  ppm: 29.8, 35.5, 51.5, 55.5, 69.6, 70.5, 109.4, 111.0, 114.0, 115.9, 117.5, 120.3, 120.7, 122.2, 123.1, 124.4, 127.4, 127.9, 128.2, 128.5, 128.6, 129.1, 131.5, 132.0, 133.8, 134.5, 136.9, 143.8, 150.8, 154.9, 154.9, 155.1, 157.8, 68.2, 169.6; FTIR (NaCl) cm<sup>-1</sup>: 3054, 2950, 2928, 2800, 1715, 1265; HRMS calcd for C<sub>46</sub>H<sub>37</sub>N<sub>3</sub>O<sub>7</sub>S (M+H<sup>+</sup>) 776.2431, (M+Na<sup>+</sup>) 798.2250, found 776.2424, 798.2218.

**5.16. Carbamic acid, ((3-(4-(((2-(3-(((*tert*-butoxy)carbonyl)-amino)propoxy)benzoyl)(6-(4-(benzyloxy)phenoxy)-2-benzothiazolyl)amino)methyl)phenoxy)propyl)carbonimidoyl)-bis-, bis(*tert*-butyl) ester (**21a**)**

The phthalimide-protected amine (**12a**) (0.255 g, 278  $\mu$ mol) in EtOH (6 mL) was treated with hydrazine hydrate (0.13 mL, 27.8  $\mu$ mol) at 68 °C for 1 h.<sup>32</sup> The solvent was removed under reduced pressure and the resulting white solid dissolved in DCM (15 mL). The organic layer was washed with saturated NaHCO<sub>3</sub> (3  $\times$  20 mL) and saturated brine. After drying (MgSO<sub>4</sub>), and filtration, the resulting amine (**20a**) was treated with 1-*H*-pyrazole-1-(*N,N'*-bis(*tert*-butoxycarbonyl)carboxamide) (86 mg, 278  $\mu$ mol) at room temperature, under N<sub>2</sub> for 96 h. Solvent was then evaporated from the reaction mixture and excess guanidylating agent was removed by radial chromatography using a 20:80 EtOAc:hexane eluant. Further purification by radial chromatography using 1:9 EtOAc:DCM as eluant afforded **21a** (0.158 g, 55%) as a clear amorphous solid. mp 51–53 °C (foam); <sup>1</sup>H NMR (300 MHz, CDCl<sub>3</sub>)  $\delta$  ppm: 1.38 (s, 9H), 1.47, 1.48 (s, 18H), 1.81 (s, 4H), 3.14 (s, 2H), 3.60 (q, 2H, *J* = 6.1 Hz), 3.97 (q, 4H, *J* = 5.6 Hz), 4.79 (s, 1H), 5.05 (s, 2H); 6.72–7.14 (m, 12H), 7.30–7.0, (m, 7H), 7.74 (m, 1H), 8.60 (t, 0.7H, *J* = 4.8 Hz), 11.48 (s, 0.7H); <sup>13</sup>C NMR (75 MHz, CDCl<sub>3</sub>)  $\delta$  ppm: 28.1, 28.3, 28.4, 28.6, 29.4, 37.5, 39.0, 51.5, 60.4, 66.2, 70.5, 79.1, 82.9, 109.3, 112.3, 114.0, 115.9, 117.5, 120.3, 120.9, 122.2, 124.7, 127.4, 127.9, 128.2, 128.5, 128.7, 129.1, 131.5, 134.5, 136.8, 143.8, 150.7, 152.9, 154.6, 154.9, 155.0, 155.8, 155.9, 157.8, 163.4, 169.5, 170.9; ATR IR(neat) cm<sup>-1</sup>: 3329, 3296, 3074, 3037, 2973, 2929, 2872, 1716, 1637, 1612; HRMS calcd for C<sub>56</sub>H<sub>66</sub>N<sub>6</sub>O<sub>11</sub>S (M+H<sup>+</sup>) 1031.4589 (M+Na<sup>+</sup>) 1053.4408, found 1031.4593, 1053.4408. For compound **20a**, MS *m/z* 789.4 (M+H<sup>+</sup>). HRMS calcd for C<sub>45</sub> H<sub>48</sub>N<sub>4</sub>O<sub>7</sub>S (M+H<sup>+</sup>) 789.3322, found 789.3321.

**5.17. Carbamic acid, ((3-(4-(((2-(3-(((*tert*-butoxy)carbonyl)-amino)propoxy)benzoyl)(6-(phenoxy)-2-benzothiazolyl)-amino)methyl)phenoxy)propyl)carbonimidoyl)-bis-, bis(*tert*-butyl) ester (**21b**)**

The title compound was prepared from **12b** in a manner similar to that described for the synthesis of **21a** to give **21b** (0.174 g, 47%) as a clear amorphous solid. mp 59–

61 °C (glass);  $^1\text{H}$  NMR (300 MHz,  $\text{CDCl}_3$ )  $\delta$  ppm: 1.39 (s, 9H), 1.48 (s, 9H), 1.49 (s, 9H), 1.86 (s, 2H), 2.02 (p, 2H,  $J = 6.9$  Hz), 3.15 (s, 2H), 3.61 (q, 2H,  $J = 6.9$  Hz), 3.97 (q, 4H,  $J = 6.0$  Hz), 4.75 (s, 1H), 5.05 (s, 1H), 5.60 (s, 1H), 6.73–7.76, 6.93–7.16, 7.29–7.46 (m, 15H), 7.79 (dd, 1H,  $J = 0.6, 8.7$  Hz);  $^{13}\text{C}$  NMR (75 MHz,  $\text{CDCl}_3$ )  $\delta$  ppm: 28.2, 28.4, 28.5, 28.7, 32.0, 37.5, 39.0, 51.6, 66.3, 66.5, 79.2, 83.0, 110.8, 112.3, 114.0, 117.9, 118.4, 122.7, 123.1, 124.7, 128.7, 128.9, 129.1, 129.6, 129.7, 131.5, 134.5, 144.3, 152.9, 153.7, 154.6, 155.9, 156.0, 157.6, 157.9, 163.4, 169.6; ATR IR(neat)  $\text{cm}^{-1}$ : 3330, 2977, 2930, 1720, 1642, 1614; HRMS calcd for  $\text{C}_{49}\text{H}_{60}\text{N}_6\text{O}_{10}\text{S}$  ( $\text{M}+\text{H}^+$ ) 925.4170, ( $\text{M}+\text{Na}^+$ ) 947.3989, found 925.4138, 947.4002.

#### 5.18. Carbamic acid, ((3-(4-(((2-methoxybenzoyl)(6-(4-benzyloxyphenoxy)-2-benzothiazolyl)amino)methyl)-phenoxy)propyl)carbonimidoyl)bis-, bis(*tert*-butyl) ester (**21c**)

The title compound was prepared from **12c** in a manner similar to that described for the synthesis of **21a** to give **21c** (0.123 g, 42%) as a clear amorphous solid. mp 55–56 °C (glass);  $^1\text{H}$  NMR (300 MHz,  $\text{CDCl}_3$ )  $\delta$  ppm: 1.49 (s, 9H), 2.05 (p, 2H,  $J = 6.0$  Hz), 3.61 (t, 2H,  $J = 6.0$  Hz), 3.74 (s, 3H), 3.97 (t, 2H,  $J = 5.9$  Hz), 5.06 (s, 2H), 5.60 (s, 1H), 6.70–7.74 (m, 20H);  $^{13}\text{C}$  NMR (75 MHz,  $\text{CDCl}_3$ )  $\delta$  ppm: 28.4, 28.7, 32.3, 39.3, 51.8, 55.8, 66.5, 70.8, 79.5, 83.3, 109.7, 111.2, 114.3, 116.2, 117.7, 120.6, 121.0, 122.5, 124.7, 127.7, 128.2, 128.6, 128.8, 128.9, 129.4, 131.7, 134.8, 137.1, 144.1, 151.1, 153.3, 155.1, 155.2, 155.5, 156.2, 158.1, 163.7, 169.9; ATR IR(neat)  $\text{cm}^{-1}$ : 3330, 3328, 3014, 3043, 2956, 2927, 2869, 1626, 1591, 1152, 1246; HRMS calcd for  $\text{C}_{49}\text{H}_{53}\text{N}_5\text{O}_9\text{S}$  ( $\text{M}+\text{H}^+$ ) 888.3642, found 888.3633.

#### 5.19. *N*-((4-(3-((Aminoiminomethyl)amino)propoxy)phenyl)methyl)-2-(3-aminopropoxy)-*N*-(6-(4-hydroxyphenoxy)-2-benzothiazolyl)benzamide (**4a**)

The substituted guanidine (**21a**) (0.153 g, 149  $\mu\text{mol}$ ) was treated with thioanisole (0.87 mL, 7.5 mmol) in TFA (3 mL) for 8 h.<sup>38</sup> The reaction was concentrated under reduced pressure and triturated repeatedly with 2:1 ethyl acetate:hexane, 2:1 ether:hexane and then hexane. De-ionised water was added and the resulting mixture was centrifuged to remove water insoluble components. The supernatant was decanted and freeze-dried to afford **4a** (78 mg, 79%) as a hygroscopic white solid.  $^1\text{H}$  NMR (300 MHz, methanol- $d_4$ )  $\delta$  ppm: 1.99 (p, 2H,  $J = 6.0$  Hz), 2.02 (p, 2H,  $J = 6.0$  Hz), 3.01 (t, 2H,  $J = 7.3$  Hz), 3.35 (t, 2H,  $J = 6.9$  Hz), 3.99 (t, 2H,  $J = 5.9$  Hz), 4.14 (t, 2H,  $J = 5.7$  Hz), 4.51 (s, 2H), 6.81–7.17 (m, 9H), 7.34 (d, 2H,  $J = 2.4$  Hz), 7.48–7.52 (m, 2H), 7.71–7.73 (dd, 2H,  $J = 0.44, 8.8$  Hz);  $^{13}\text{C}$  NMR (75 MHz, methanol- $d_4$ )  $\delta$  ppm: 29.0, 30.5, 39.4, 40.4, 53.7, 66.9, 67.7, 110.6, 114.5, 116.3, 118.1, 119.4, 122.7, 123.2, 124.2, 126.4, 130.0, 130.5, 131.4, 134.1, 136.6, 145.6, 151.6, 156.0, 156.7, 158.5, 160.5, 172.6; ATR IR(neat)  $\text{cm}^{-1}$ : 3359, 3200, 2930, 1673, 1599; HRMS

calcd for  $\text{C}_{34}\text{H}_{36}\text{N}_6\text{O}_5\text{S}$  ( $\text{M}+\text{H}^+$ ) 641.2546, found 641.2534.

#### 5.20. *N*-((4-(3-((Aminoiminomethyl)amino)propoxy)phenyl)methyl)-2-(3-aminopropoxy)-*N*-(6-phenoxy-2-benzothiazolyl)benzamide (**4b**)

The substituted guanidine (**21b**) (55.1 mg, 59.6  $\mu\text{mol}$ ) was treated with TFA (0.18 mL, 2.4 mmol) in DCM (3 mL) for 6 h. The reaction was concentrated under reduced pressure and then exposed to high vacuum to remove any remaining TFA. The dirty green product was dissolved in water, centrifuged and the supernatant decanted. Freeze-drying of the supernatant afforded **4b** (44.9 mg, 79%) as a hygroscopic white solid.  $^1\text{H}$  NMR (300 MHz, methanol- $d_4$ )  $\delta$  ppm: 2.06 (p, 4H,  $J = 6.6$  Hz), 3.06 (t, 2H,  $J = 7.2$  Hz), 3.39 (t, 2H,  $J = 6.75$  Hz), 4.03 (t, 2H,  $J = 5.85$  Hz), 4.17 (t, 2H,  $J = 5.55$  Hz), 5.43 (s, 2H), 6.83 (m, 2H), 6.94–7.20 (m, 9H), 7.30–7.60 (m, 5H), 7.84 (d,  $J = 9.0$  Hz);  $^{13}\text{C}$  NMR (75 MHz, methanol- $d_4$ )  $\delta$  ppm: 29.0, 30.5, 39.4, 40.4, 53.7, 66.9, 67.7, 112.6, 114.5, 116.3, 120.5, 120.6, 123.2, 124.4, 125.4, 126.4, 130.0, 130.5, 131.4, 131.7, 134.1, 136.7, 146.4, 156.7, 159.9, 172.6; ATR IR(neat)  $\text{cm}^{-1}$ : 3355, 3172, 2962, 1671, 1595; MS  $m/z$  625 ( $\text{M}+\text{H}^+$ ), 739 ( $\text{M}+\text{TFA}^+$ ); MS (ESI $^-$ )  $m/z$  851 ( $\text{M}+2\text{TFA}-\text{H}^-$ ); HRMS calcd for  $\text{C}_{34}\text{H}_{36}\text{N}_6\text{O}_4\text{S}$  ( $\text{M}+\text{H}^+$ ) 625.2597, ( $\text{M}+\text{TFA}+\text{H}^+$ ) 739.2527, found 625.2587, 739.2517.

#### 5.21. *N*-((4-(3-((Aminoiminomethyl)amino)propoxy)phenyl)methyl)-*N*-(6-(4-hydroxyphenoxy)-2-benzothiazolyl)-2-methoxybenzamide (**4c**)

The title compound was prepared from **21c** in a manner similar to that described for the synthesis of **4a**, this time using a reaction time of 6 h to give **4c** (16.9 mg, 70%) as a hygroscopic white solid.  $^1\text{H}$  NMR (300 MHz, methanol- $d_4$ )  $\delta$  ppm: 2.02 (p, 2H,  $J = 6.3$  Hz), 3.39 (t, 2H,  $J = 6.8$  Hz), 3.79 (s, 3H), 4.04 (t, 2H,  $J = 6.0$  Hz), 6.76–7.75 (m, 15H);  $^{13}\text{C}$  NMR (75 MHz, methanol- $d_4$ )  $\delta$  ppm: 30.5, 40.5, 53.5, 57.1, 66.9, 110.7, 113.4, 116.2, 118.2, 119.3, 121.1, 122.7, 124.1, 127.5, 130.2, 130.4, 131.6, 134.0, 136.6, 145.7, 151.7, 115.9, 157.8, 158.3, 160.3, 172.6;  $^{13}\text{C}$  NMR (acetone- $d_6$ )  $\delta$  ppm: 39.9, 52.8, 56.8, 66.3, 110.5, 112.9, 115.7, 117.7, 118.6, 122.1, 122.2, 123.6, 126.0, 129.8, 129.9, 130.9, 133.2, 135.9, 145.2, 150.9, 155.3, 156.9, 157.2, 159.5, 170.7; ATR IR(neat)  $\text{cm}^{-1}$ : 3353, 3190, 2922, 2857, 1657, 1631, 1599; MS  $m/z$  598 ( $\text{M}+\text{H}^+$ ); MS (ESI $^-$ )  $m/z$  596 ( $\text{M}-\text{H}^-$ ); HRMS calcd for  $\text{C}_{32}\text{H}_{31}\text{N}_5\text{O}_5\text{S}$  ( $\text{M}+\text{H}^+$ ) 598.2124, found 598.2115.

#### 5.22. 2-(3-Aminopropoxy)-*N*-((4-(3-aminopropoxy)phenyl)methyl)-*N*-(6-(4-hydroxyphenoxy)-2-benzothiazolyl)-benzamide (**4d**)

The amine (**20a**) (57 mg, 62.2  $\mu\text{mol}$ ) obtained using the same hydrazinolysis procedure described above in the preparation of **21a**, was treated with thioanisole (0.36 mL, 3.1 mmol) in TFA (0.8 mL) for 3 h. The reaction mixture was then concentrated under reduced

pressure and triturated repeatedly with 2:1 ethyl acetate:hexane, 2:1 ether:hexane and then hexane. The crude product was triturated with water and centrifuged to remove water insoluble components. The supernatant was decanted and freeze-dried to afford **4d** (28 mg, 75%) as a hygroscopic white solid.  $^1\text{H}$  NMR (300 MHz, methanol- $d_4$ )  $\delta$  ppm: 2.13 (p, 4H,  $J = 6.2$  Hz), 3.06 (t, 2H,  $J = 7.4$  Hz), 3.14 (t, 2H,  $J = 6.9$  Hz), 4.07 (t, 2H,  $J = 5.7$  Hz), 4.18 (t, 2H,  $J = 5.4$  Hz), 6.81–7.38 (m, 13H), 7.50–7.88 (m, 2H);  $^{13}\text{C}$  NMR (75 MHz, methanol- $d_4$ )  $\delta$  ppm: 29.0, 29.2, 39.4, 39.4, 53.6, 67.1, 67.7, 110.6, 114.5, 116.3, 118.2, 119.4, 122.7, 123.2, 124.2, 126.4, 130.2, 130.5, 131.5, 134.1, 136.6, 145.6, 151.6, 156.0, 156.7, 158.5, 160.2, 172.6; ATR IR(neat)  $\text{cm}^{-1}$ : 3062, 3036, 2953, 1670, 1600; HRMS calcd for  $\text{C}_{33}\text{H}_{34}\text{N}_4\text{O}_5\text{S}$  ( $\text{M}+\text{H}^+$ ) 599.2328, found 599.2346.

### 5.23. Biological methods

Peptide synthesis, radiolabelling of the peptides with  $^{125}\text{I}$  and rat brain preparation were conducted following previously described procedures.<sup>39</sup> Radioligand binding assays were run in triplicate in 96-well plates at room temperature.<sup>42–44</sup> The first three wells of the 96-well plate (Polystyrene, Round bottom, Nunc<sup>TM</sup>, Denmark) contained 0.6  $\mu\text{M}$  of compound (total of seven dilutions, 1:10), 5–10 fmol of radiolabelled peptide ( $^{125}\text{I}$ -GVIA) and 8  $\mu\text{g}$  of crude rat membrane (added last). All dilutions were made in assay buffer (20 mM HEPES, 75 mM NaCl, 0.2 mM EDTA, 0.2 mM EGTA, 2  $\mu\text{M}$  Leupeptin, 2  $\mu\text{L}$  apoprotinin (to 30 mL assay buffer), 0.1% BSA, pH 7.4) and the final volume in each well was 150  $\mu\text{L}$ . The plate was left on a shaker for 1 h at room temperature before being filtered. The incubation period was terminated by washing the plate with wash buffer (20 mM HEPES, 125 mM NaCl, pH 7.4) and filtering under vacuum (Tomtec). The glass fibre filter used (90  $\times$  120 mm, double thickness, Wallac, Finland) was soaked in 0.6% polyethyleneimine immediately prior to filtering to reduce nonspecific binding. The filter was put in a Sample Bag (Wallac, Finland) containing 8 mL BetaPlate Scint (Wallac, Finland) and the radioactivity bound to the filter was counted using a 1450 MicroBeta Wallac Jet (Wallac, Finland). The data was analysed using GraphPad Prism 2.0 (GraphPad Software, Inc, San Diego, USA).

### Acknowledgements

Financial support of this work was provided by the Biomolecular Research Institute, the National Health and Medical Research Council of Australia and Monash University. Y.P.L. is a recipient of a Monash Graduate Scholarship and an International Postgraduate Research Scholarship. C.I.S. is a recipient of a University of Queensland International Postgraduate Research Scholarship and a Graduate Scholarship from the Institute for Molecular Bioscience.

### References and notes

- Baell, J. B.; Duggan, P. J.; Lok, Y. P. *Aust. J. Chem.* **2004**, *57*, 179.
- Olivera, B. M.; Miljanich, G. P.; Ramachandran, J.; Adams, M. E. *Annu. Rev. Biochem.* **1994**, *63*, 823.
- (a) Alewood, P.; Hopping, G.; Armishaw, C. *Aust. J. Chem.* **2003**, *56*, 769; (b) Terlau, H.; Olivera, B. M. *Physiol. Rev.* **2004**, *84*, 41.
- Jones, R. M.; Bulaj, G. *Curr. Pharm. Des.* **2000**, *6*, 1249.
- M<sup>c</sup>Intosh, J. M.; Jones, R. M. *Toxicon* **2001**, *39*, 1447.
- Olivera, B. M.; Cruz, L. J. *Toxicon* **2001**, *39*, 7.
- The alternative designation for the N-type VGCC,  $\text{Ca}_v2.2$ , is derived from a nomenclature system based on structural aspects of the channels, similar to that used for potassium channels: Ertel, E. A.; Campbell, K. P.; Harpold, M. M.; Hofmann, F.; Mori, Y.; Perez-Reyes, E.; Schwartz, A.; Snutch, T. P.; Tanabe, T.; Birnbaumer, L.; Tsien, R. W.; Catterall, W. A. *Neuron* **2000**, *25*, 533.
- Lipton, P. *Physiol. Rev.* **1999**, *79*, 1431.
- Morley, P.; Tauskela, J. S.; Hakim, A. M. Calcium Overload in Cerebral Ischemia Molecular and Cellular Pathophysiology. In *Cerebral Ischemia: Molecular and Cellular Pathology*; Walz, W., Ed.; Humana: New Jersey, 1999.
- Nelson, R. M.; Lambert, D. G.; Green, A. R.; Hainsworth, A. H. *Brain Res.* **2003**, *964*, 1.
- Adams, D. J.; Alewood, P. F.; Craik, D. J.; Drinkwater, R. D.; Lewis, R. J. *Drug. Dev. Res.* **1999**, *46*, 219.
- Cox, B. *Curr. Rev. Pain* **2000**, *4*, 488.
- Miljanich, G. P.; Ramachandran, J. *J. Annu. Rev. Pharmacol. Toxicol.* **1995**, *35*, 707.
- Nielsen, K. J.; Schroeder, T.; Lewis, R. J. *Mol. Recognit.* **2000**, *13*, 55.
- Atanassoff, P. G.; Hartmannsgruber, M. W.; Thrasher, J.; Wermeling, D.; Longton, W.; Gaeta, R.; Singh, T.; Mayo, M.; McGuire, D.; Luther, R. R. *Reg. Anesth. Pain Med.* **2000**, *25*, 274.
- Staats, P. S.; Yearwood, T.; Charapata, S. G.; Presley, R. W.; Wallace, M. S.; Bryas-Smith, M.; Fisher, R.; Bryce, D. A.; Mangieri, E. A.; Luther, R. R.; Mayo, M.; M<sup>c</sup>Guire, D.; Ellis, D. *JAMA* **2004**, *291*, 63.
- Pallaghy, P. K.; Norton, R. S. *J. Peptide Res.* **1998**, *53*, 343.
- Cruz, L. J.; Olivera, B. M. *J. Biol. Chem.* **1986**, *261*, 6230.
- Flinn, J. P.; Pallaghy, P. K.; Lew, M. J.; Murphy, R.; Angus, J. A.; Norton, R. S. *Eur. J. Biochem.* **1999**, *262*, 447.
- Lew, M. J.; Flinn, J. P.; Pallaghy, P. K.; Murphy, R.; Whorlow, S. L.; Wright, C. E.; Norton, R. S.; Angus, J. A. *J. Biol. Chem.* **1997**, *272*, 12014.
- Norton, R. S.; Pallaghy, P. K.; Baell, J. B.; Wright, C. E.; Lew, M. J.; Angus, J. A. *Drug Dev. Res.* **1999**, *46*, 206.
- Guo, Z.-X.; Cammidge, A. N.; Horwell, D. C. *Tetrahedron* **2000**, *56*, 5169.
- Menzler, S.; Bikker, J. A.; Horwell, D. C. *Tetrahedron Lett.* **1998**, *39*, 7619.
- Menzler, S.; Bikker, J. A.; Suman-Chauhan, N.; Horwell, D. C. *Bioorg. Med. Chem. Lett.* **2000**, *10*, 345.
- Dabak, K. *Turk. J. Chem.* **2002**, *26*, 955.
- Baell, J. B.; Forsyth, S. A.; Gable, R. W.; Norton, R. S.; Mulder, R. J. *J. Comput. Aided Mol. Des.* **2001**, *15*, 1119.
- Kim, J. I.; Takahashi, M.; Ogura, A.; Kohno, T.; Kudo, Y.; Sato, K. *J. Biol. Chem.* **1994**, *269*, 23876.
- Bowersox, S. S.; Valentino, K. L.; Luther, R. R. *Drugs News Perspect.* **1994**, *7*, 261.
- Lau, A. N. K.; Vo, L. P.; Fone, M. M.; Duff, D. W.; Merlino, G. *J. Polym. Sci. Part A: Polym. Chem.* **1994**, *32*, 1507.
- Nagarajan, K.; Hendi, S. B.; Goud, A. N.; Sen, H. G.; Deb, B. N. *Ind. J. Pharm. Sci.* **1991**, *48*, 85.

31. Dick, D. L.; Rao, T. V. S.; Sukumaran, D.; Lawrence, D. S. *J. Am. Chem. Soc.* **1992**, *114*, 2664.
32. Manka, J. S.; Lawrence, D. S. *J. Am. Chem. Soc.* **1990**, *112*, 2440.
33. Osby, J. O.; Martin, M. G.; Ganem, B. *Tetrahedron Lett.* **1984**, *25*, 2093.
34. Kaduk, C.; Wenschuh, H.; Beyermann, J.; Forner, K.; Carpino, L. A.; Bienert, M. *Lett. Peptide Sci.* **1995**, *2*, 285.
35. Fisher, M. J.; Gunn, B.; Harms, C. S.; Kline, A. D.; Mullaney, J. T.; Nunes, A.; Scarborough, R. M.; Arfsten, A. E.; Skelton, M. A.; Um, S. L.; Utterback, B. G.; Jakuboswki, J. A. *J. Med. Chem.* **1997**, *40*, 2085.
36. Drake, B.; Patek, M.; Labl, M. *Synthesis* **1994**, 579.
37. Nudelman, A.; Bechor, Y.; Falb, E.; Fischer, B.; Wexler, W. A.; Nudelman, A. *Synth. Commun.* **1998**, *28*, 471.
38. Kiso, Y.; Ukawa, K.; Nakamura, S.; Ito, K.; Akita, T. *Chem. Pharm. Bull.* **1980**, *28*, 673.
39. Nielsen, K. J.; Adams, D. A.; Alewood, P. F.; Lewis, R. J.; Thomas, L.; Schroeder, T.; Craik, D. *Biochemistry* **1999**, *38*, 6741.
40. Williams, D. H.; Westwell, M. S. *Chem. Soc. Rev.* **1998**, *27*, 57.
41. Lee, B. H.; Miller, M. J. *J. Org. Chem.* **1983**, *48*, 24.
42. Kristipati, R.; Nadasdi, L.; Tarczy-Hornoch, K.; Lau, K.; Miljanich, G. P.; Ramachandran, J.; Bell, J. R. *Mol. Cell Neurosci.* **1994**, *5*, 219.
43. Lewis, R. J.; Nielsen, K. J.; Craik, D. J.; Loughnan, M. L.; Adams, D. A.; Sharpe, I. A.; Luchian, T.; Adams, D. J.; Bond, T.; Thomas, L.; Jones, A.; Matheson, J. L.; Drinkwater, R.; Andrews, P. R.; Alewood, P. F. *J. Biol. Chem.* **2000**, *275*, 35335.
44. Nadasdi, L.; Yamashiro, D.; Chung, D.; Tarczy-Hornoch, K.; Adriaenssens, P.; Ramachandran, J. *Biochemistry* **1995**, *34*, 8076.